2011 International Nuclear Atlantic Conference - INAC 2011
Belo Horizonte,MG, Brazil, October 24-28, 2011
ASSOCIAÇÃO BRASILEIRA DE ENERGIA NUCLEAR - ABEN
ISBN: **978-85-99141-04-5**

COMPUTATIONAL MODELING FOR THE ANGULAR RECONSTRUCTION OF MONOENERGETIC NEUTRON FLUX IN NON-MULTIPLYING SLABS USING SYNTHETIC DIFFUSION APPROXIMATION

[1]Ralph S. Mansur and [2]Ricardo C. Barros

Programa de Pós-graduação em Ciências Computacionais
Instituto de Matemática e Estatística
Universidade do Estado do Rio de Janeiro
Rua São Francisco Xavier 524
28630-050 Rio de Janeiro, RJ
[1]ralph@ime.uerj.br , [2]rcbarros@pq.cnpq.br

ABSTRACT

We describe a method to determine the neutron scalar flux in a slab using monoenergetic diffusion model. To achieve this goal we used three ingredients in the computational code that we developed on the Scilab plataform: (i) a spectral nodal method that generates numerical solution for the one-speed slab-geometry fixed-source diffusion problem with no spatial truncation errors; (ii) a spatial reconstruction scheme to yield detailed profile of the coarse-mesh solution; and (iii) an angular reconstruction scheme to yield approximately the neutron angular flux profile at a given location of the slab migrating in a given direction. Numerical results are given to illustrate the efficiency of the offered code.

1. INTRODUCTION

In this paper we describe two analytical reconstruction schemes for the coarse-mesh numerical solution generated by the spectral nodal method for fixed-source one-speed diffusion problems in slab geometry [1]. That is, the spatial reconstruction scheme expresses the diffusion solution in each spatial cell as a linear combination of two elementary solutions, that we determine by spectral analysis, and assigns boundary conditions at cell edges, that are given by the spectral nodal results to obtain a system of two linear algebraic equations in two unknown expansion coefficients, which then yield the exact diffusion solution at each point in the cell, since the spectral nodal method for diffusion (SND) is free from all spatial truncation errors. Moreover, the angular reconstruction scheme yields approximate angular flux at any angular direction $-1 \leq \mu \leq 1$, except $\mu = 0$, where $\mu = \cos \theta$, with θ being defined as the polar angle [2]. To achieve this goal, we substitute the local solution within each cell of the spatial grid, as we determine by the spatial reconstruction scheme, into the integral source terms of the analytical first-order form of neutron transport equation in slab geometry with isotropic scattering [2] and solve the resulting approximate differential equation analytically.

Now we outline the content of the remainder of this paper: in the next section we describe the spatial and the angular reconstruction schemes of the SND coarse-mesh solution. In section 3 we present numerical results to a multilayer fixed source problem in slab geometry, and we conclude with a brief discussion in section 4.

2. THE SPATIAL AND THE ANGULAR RECONSTRUCTION SCHEMES OF THE SND COARSE-MESH NUMERICAL SOLUTION

2.1. The Spatial Reconstruction Scheme

Let us consider Fig.1 which represents a spatial discretization cell, also termed node Ω_i with the scalar fluxes as generated by the SND method, which is free from spatial truncation errors. At this point we remark that the cell-edges have been defined as $x_{i-1/2} = 0$ and $x_{i+1/2} = h_i$, $i = 1 : I$, to avoid finite arithmetic overflow in coarse spatial grids as we need to evaluate exponential functions with positive exponents, as we describe next.

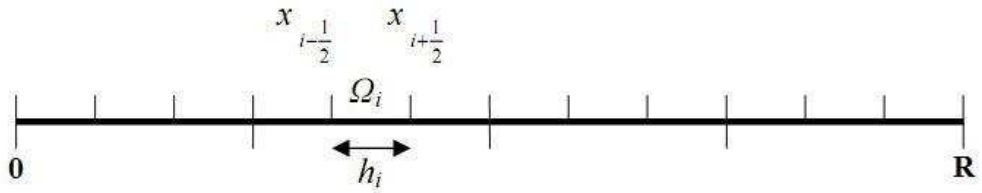

Figure 1. Spatial node Ω_i of width h_i with the scalar flux as generated by the SND method.

To describe the spectral analysis we perform to the diffusion equation inside node Ω_i in order to obtain the SND method, it is convenient to write the one-speed slab-geometry diffusion equation in Ω_i in the following form:

$$\frac{d}{dx} J(x) + \Sigma_{ai}\, \phi(x) = Q_i \tag{1}$$

$$J(x) = -D_i \frac{d}{dx} \phi(x), \quad 0 \le x \le R \ , \tag{2}$$

where R represents the slab length, and

$\phi(x)$: neutron scalar flux;
$J(x)$: total current;
Σ_{ai} : absorption macroscopic cross section;
D_i : diffusion coefficient;
Q_i : uniform and isotropic interior source;

Now we apply the operator $\frac{1}{h_i} \int_{x_{i-\frac{1}{2}}}^{x_{i+\frac{1}{2}}} dx$ to Eqs. (1) and (2) to obtain the discretized diffusion

balance equations

$$\begin{cases} \dfrac{J_{i+\frac{1}{2}} - J_{i-\frac{1}{2}}}{h_i} + \Sigma_{ai}\,\overline{\phi}_i = Q_i & (3) \\ \overline{J}_i = -\dfrac{D_i}{h_i}\left(\phi_{i+\frac{1}{2}} - \phi_{i-\frac{1}{2}}\right) \quad . & (4) \end{cases}$$

Here we have defined the average values within the spatial cell Ω_i as

$$\overline{g}_i = \frac{1}{h_i}\int_{x_{1-\frac{1}{2}}}^{x_{1+\frac{1}{2}}} g(x)\,dx \quad , \quad g = J \text{ or } \phi \quad . \tag{5}$$

Now we write the expressions for the general solution of Eqs. (1) and (2) in Ω_i as

$$\phi(x) = a\,e^{-\Sigma_a x/\nu} + \phi^p \quad , \tag{6}$$

$$J(x) = b\,e^{-\Sigma_a x/\nu} + J^p \quad , \tag{7}$$

where the superscript p denotes the particular solution. Now we substitute Eqs. (6) and (7) into Eqs. (1) and (2) to obtain the following system of two linear algebraic equations:

$$\begin{cases} \Sigma_a\left(a\,e^{-\frac{\Sigma_a x}{\nu}}\right) - \dfrac{\Sigma_a}{\nu}\left(b\,e^{-\frac{\Sigma_a x}{\nu}}\right) = Q - \Sigma_a\,\phi^p & (8) \\ -\dfrac{D\Sigma_a}{\nu}\left(a\,e^{-\frac{\Sigma_a x}{\nu}}\right) + b\,e^{-\frac{\Sigma_a x}{\nu}} = -J^p \quad . & (9) \end{cases}$$

We determine the particular solutions by setting the right-hand sides of Eqs. (8) and (9) equal to zero. Therefore, we obtain

$$\phi^p = \frac{Q}{\Sigma_a} \quad , \tag{10}$$

$$J^p = 0 \quad . \tag{11}$$

By solving the resulting homogeneous system for non-trivial solution, we obtain

$$\nu = \pm\sqrt{D\Sigma_a} \quad . \tag{12}$$

As it stands, the expressions for the elementary solutions of Eqs. (1) and (2) appear as

$$\phi(x) = a\, e^{-\sqrt{\frac{\Sigma_a}{D}}\,x} + \frac{Q}{\Sigma_a} \quad , \tag{13}$$

$$J(x) = b\, e^{-\sqrt{\frac{\Sigma_a}{D}}\,x} \quad . \tag{14}$$

Furthermore, the undetermined homogeneous system is given by

$$\begin{cases} \Sigma_a\, a - \sqrt{\dfrac{\Sigma_a}{D}}\, b = 0 & (15) \\ -\sqrt{D\Sigma_a}\, a + b = 0 \quad . & (16) \end{cases}$$

By choosing a = 1, we obtain

$$b = \sqrt{D\,\Sigma_a} \quad , \tag{17}$$

and Eqs. (13) and (14) can be written as

$$\phi(x) = e^{-\sqrt{\frac{\Sigma_a}{D}}\,x} + \frac{Q}{\Sigma_a} \quad , \tag{18}$$

$$J(x) = \sqrt{D\Sigma_a}\, e^{-\sqrt{\frac{\Sigma_a}{D}}\,x} \quad . \tag{19}$$

Therefore, the expressions for the analytical general solutions of Eqs. (1) and (2) appear as

$$\phi(x) = C_1\, e^{-\sqrt{\frac{\Sigma_a}{D}}\,x} + C_2\, e^{\sqrt{\frac{\Sigma_a}{D}}\,x} + \frac{Q}{\Sigma_a} \quad , \tag{20}$$

$$J(x) = C_1\sqrt{D\Sigma_a}\, e^{-\sqrt{\frac{\Sigma_a}{D}}\,x} + C_2\sqrt{D\Sigma_a}\, e^{\sqrt{\frac{\Sigma_a}{D}}\,x} \quad , \; x \in \Omega_i \quad . \tag{21}$$

Now we write two auxiliary equations in the form

$$\bar{\phi}_i = \frac{\gamma_i}{2}\left(\phi_{i+\frac{1}{2}} + \phi_{i-\frac{1}{2}} \right) + G(Q_i) \quad , \tag{22}$$

$$\bar{J}_i = \frac{\beta_i}{2}\left(J_{i+\frac{1}{2}} + J_{i-\frac{1}{2}} \right) \quad . \tag{23}$$

In order to determine expressions for γ_i and β_i , we first substitute Eq. (18) into Eq. (22). By using definition (5) and defining the diffusion length

$$L_i = \sqrt{\frac{D_i}{\Sigma_{ai}}} \quad , \tag{24}$$

we obtain

$$\bar{\phi}_i = \frac{L_i}{h_i}\left(e^{-\frac{x_{i-\frac{1}{2}}}{L_i}} - e^{-\frac{x_{i+\frac{1}{2}}}{L_i}} \right) + \frac{Q}{\Sigma_a} \quad , \tag{25}$$

which can be substituted into the auxiliary equation (22) to obtain the following expression for $G(Q_i)$:

$$G(Q_i) = \frac{(1-\gamma_i)Q_i}{\Sigma_{ai}} \quad , \tag{26}$$

and the following expression for γ_i :

$$\gamma_i = 2\frac{L_i}{h_i}\tanh\left(\frac{h_i}{2L_i}\right) \quad . \tag{27}$$

Following similar procedure, we obtain the expression for β_i which is identical to the expression (27). Therefore, the auxiliary equations (22) and (23) appear as

$$\begin{cases} \bar{\phi}_i = \dfrac{\gamma_i}{2}\left(\phi_{i+\frac{1}{2}} + \phi_{i-\frac{1}{2}} \right) + \dfrac{(1-\gamma_i)Q_i}{\Sigma_{ai}} \quad , & (28) \\ \bar{J}_i = \dfrac{\gamma_i}{2}\left(J_{i+\frac{1}{2}} + J_{i-\frac{1}{2}} \right) \quad . & (29) \end{cases}$$

Now, we substitute Eqs. (28) and (29) into Eqs. (3) and (4) to obtain

$$\begin{cases} J_{i+\frac{1}{2}} - J_{i-\frac{1}{2}} = h_i\gamma_i Q_i - \dfrac{h_i\gamma_i\Sigma_{ai}}{2}\left(\phi_{i+\frac{1}{2}} + \phi_{i-\frac{1}{2}} \right) \quad , & (30) \\ J_{i+\frac{1}{2}} + J_{i-\frac{1}{2}} = -\dfrac{2D_i}{h_i\gamma_i}\left(\phi_{i+\frac{1}{2}} + \phi_{i-\frac{1}{2}} \right) \quad . & (31) \end{cases}$$

By summing Eqs. (30) and (31) and subtracting Eq. (30) from Eq. (31) we obtain respectively

$$J_{i+\frac{1}{2}} = -\frac{D_i}{h_i \gamma_i}\left(\phi_{i+\frac{1}{2}} - \phi_{i-\frac{1}{2}}\right) - \frac{h_i \gamma_i \Sigma_{ai}}{4}\left(\phi_{i+\frac{1}{2}} + \phi_{i-\frac{1}{2}}\right) + \frac{h_i \gamma_i}{2} Q_i \quad , \tag{32}$$

$$J_{i-\frac{1}{2}} = -\frac{D_i}{h_i \gamma_i}\left(\phi_{i+\frac{1}{2}} - \phi_{i-\frac{1}{2}}\right) + \frac{h_i \gamma_i \Sigma_{ai}}{4}\left(\phi_{i+\frac{1}{2}} + \phi_{i-\frac{1}{2}}\right) - \frac{h_i \gamma_i}{2} Q_i \quad . \tag{33}$$

By substituting (i+1) into the subscript i in Eq. (33), we write

$$J_{i+\frac{1}{2}} = -\frac{D_{i+1}}{h_{i+1} \gamma_{i+1}}\left(\phi_{i+\frac{3}{2}} - \phi_{i+\frac{1}{2}}\right) + \frac{h_{i+1} \gamma_{i+1} \Sigma_{ai+1}}{4}\left(\phi_{i+\frac{3}{2}} + \phi_{i+\frac{1}{2}}\right) - \frac{h_{i+1} \gamma_{i+1}}{2} Q_{i+1} \quad . \tag{34}$$

By comparing Eqs. (32) and (34), we obtain an equation involving three consecutive node-edge scalar fluxes on the left-hand side, and the sources Q_i and Q_{i+1} on the right-hand side. This equation is used for the nodes Ω_i , i = 2 : I+1 .

For the first spatial cell, by setting i = 1 in Eq. (33), we obtain

$$J_{\frac{1}{2}} = -\frac{D_1}{h_1 \gamma_1}\left(\phi_{\frac{3}{2}} - \phi_{\frac{1}{2}}\right) + \frac{h_1 \gamma_1 \Sigma_{a1}}{4}\left(\phi_{\frac{3}{2}} + \phi_{\frac{1}{2}}\right) - \frac{h_1 \gamma_1}{2} Q_1 \quad . \tag{35}$$

Furthermore, we introduce the generalized left boundary condition as

$$J_{\frac{1}{2}} = I_0 - \alpha_0 \phi_{\frac{1}{2}} \quad . \tag{36}$$

Using Eq. (36) into Eq. (35), we obtain an equation involving $\phi_{1/2}$ and $\phi_{3/2}$ on the left-hand side, and the source Q_1 and I_0 on the right-hand side. This equation is used for the first spatial cell, i.e. , Ω_1 .

For the last spatial cell, we set i = I in Eq. (32), and we obtain

$$J_{I+\frac{1}{2}} = -\frac{D_I}{h_I \gamma_I}\left(\phi_{I+\frac{1}{2}} - \phi_{I-\frac{1}{2}}\right) - \frac{h_I \gamma_I \Sigma_{aI}}{4}\left(\phi_{I+\frac{1}{2}} + \phi_{I-\frac{1}{2}}\right) + \frac{h_I \gamma_I}{2} Q_I \quad . \tag{37}$$

Furthermore, we substitute the generalized boundary condition at x = R as given by

$$J_{I+\frac{1}{2}} = \alpha_R \phi_{I+\frac{1}{2}} - I_R \tag{38}$$

into Eq. (37). The result involves $\phi_{I+\frac{1}{2}}$ and $\phi_{I-\frac{1}{2}}$ on the left-hand side, and the source Q_I and I_L on the right-hand side. This equation is used for the last spatial cell, i.e. , Ω_I .

The parameters α_m and I_m , $m \in \{0, R\}$, depend on the boundary conditions. They are given in accordance with Table 1.

Table 1. Boundary conditions

	Prescribed	Vacuum	Reflexive	Zero scalar-flux
α_m	0.5	0.5	0	10^{10}
I_m	I[a]	0	0	0

a. Input data.

The expressions for the interior interfaces, first and last spatial cells give an algebraic linear system with I+1 equations for the I+1 unknowns ϕ_j, j = ½ : I + ½. The coefficient matrix of this linear system is symmetric, tridiagonal and has the characteristic of being diagonal dominant, which discards the use of pivoting techniques to solve the system for the scalar flux at the node edges [3].

The numerical solution generated by the SND method has no spatial truncation errors. Therefore, it generates accurate numerical results even for coarse discretization grids set up on the domain.

To proceed further with the spatial reconstruction scheme, we first set $x_{i-\frac{1}{2}} = 0$ and then $x_{i+\frac{1}{2}} = h_i$, i = 1 : I , in Eq. (20) of the analytical solution inside Ω_i . As the values of $\phi(0)$ and $\phi(h_i)$ have been determined previously by the SND method, we can solve the system

$$\begin{cases} \phi(0) = C_1 + C_2 + \dfrac{Q_i}{\Sigma_{ai}} \\ \phi(h_i) = C_1 e^{-\frac{h_i}{L_i}} + C_2 e^{\frac{h_i}{L_i}} + \dfrac{Q_i}{\Sigma_{ai}} \end{cases} , \tag{39}$$

for the two unknowns C_1 and C_2 .

To conclude the spatial reconstruction scheme, we substitute the constants C_1 and C_2 back into the local general solution (20), so we can evaluate the scalar flux at any point $x \in \Omega_i$. At this point we remark that all spatial cells of the same material zone that have the same width may have different set of constants C_1 and C_2 , as the right-hand side of system (20) is generally different in each Ω_i, as it depends on the coarse-mesh solution generated by the SND method in accordance with Eq. (39).

2.2. The Angular Reconstruction Scheme

Once we have described an algorithm to perform spatial reconstruction within each spatial node Ω_i , i = 1 : I, of the coarse-mesh discretization grid, we proceed to describing an algorithm to perform angular reconstructions for any possible value (except $\mu = 0$) of the direction-of-motion variable μ ($-1 \leq \mu \leq 1$).

The neutron transport equation in slab geometry with isotropic scattering can be written as

$$\mu \frac{\partial}{\partial x}\psi(x,\mu)+\Sigma_T \psi(x,\mu)=\frac{1}{2}\Sigma_s \int_{-1}^{+1}\psi(x,\mu')d\mu'+\frac{Q}{2} \quad , \tag{40}$$

where

$\psi(x,\mu)$: neutron angular flux in direction μ ;
Σ_T : total macroscopic cross section;
Σ_s : scattering macroscopic cross section.

The total macroscopic cross section is defined [2] by

$$\Sigma_T = \frac{1}{3D} \quad . \tag{41}$$

Therefore, let us use the standard definition of neutron scalar flux

$$\phi(x)=\int_{-1}^{+1}\psi(x,\mu')d\mu' \quad . \tag{42}$$

Moreover, using the expression for the local general solutions (20) in Eq. (40), we solve the resulting equation analytically for the neutron angular flux $\psi(x,\mu)$, $x \in \Omega_i$. For $0 < \mu \leq 1$, the result is

$$\psi(x,\mu)=\psi(0,\mu)e^{-\Sigma_{Ti}x/\mu}+\frac{\Sigma_{si}}{2\mu}\sum_{\ell=1}^{2}\frac{c_\ell\left(e^{-\Sigma_{Ti}x/\mu}-e^{-\Sigma_{ai}x/\nu_\ell}\right)}{\frac{\Sigma_{ai}}{\nu_\ell}-\frac{\Sigma_{Ti}}{\mu}}+\frac{Q_i}{2\Sigma_{ai}}\left(1-e^{-\Sigma_{Ti}x/\mu}\right) \quad . \tag{43}$$

Furthermore, for $-1 \leq \mu < 0$, we obtain the result

$$\psi(x,\mu)=\psi(h_i,\mu)e^{-\Sigma_{Ti}(h_i-x)/|\mu|}+\frac{\Sigma_{si}}{2|\mu|}\sum_{\ell=1}^{2}\frac{C_\ell\left(e^{-\Sigma_{ai}x/\nu_\ell}-e^{-\Sigma_{ai}h_i/\nu_\ell}e^{-\Sigma_{Ti}(h_i-x)/|\mu|}\right)}{\frac{\Sigma_{ai}}{\nu_\ell}+\frac{\Sigma_{Ti}}{|\mu|}}+$$

$$+\frac{Q_i}{2\Sigma_{ai}}\left(1-e^{-\Sigma_{Ti}(h_i-x)/|\mu|}\right) \quad . \tag{44}$$

Here, x = 0 is the left-hand side edge of node Ω_i and x = h_i is the right-hand side edge of node Ω_i, i.e., $0 \le x \le h_i$.

Equations (43) and (44) are the analytical solutions of the approximate neutron transport equation for all direction-of-motion variables $-1 \le \mu \le 1.$, $\mu \neq 0$, wherein we have considered the local general solution for the scalar flux given by Eqs. (20). We remark that the values of C_ℓ are determined by solving the linear system (39), as described for the spatial reconstruction scheme. Moreover, we see in Eqs. (43) and (44) that the present angular reconstruction scheme is not valid for the particular case of $\mu = 0$.

3. NUMERICAL RESULTS

We consider a heterogeneous model problem that consists of a three-layer slab of thickness R = 25cm and two material zones, represented in Fig.2. Vacuum boundary conditions apply at x = 0 and x = 25. The central layer has a constant unit source and the cross sections for the two material zones are listed in Table 2.

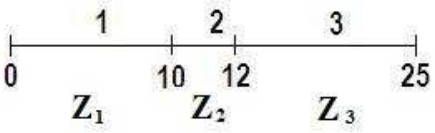

Figure 2. Model Problem.

Table 2. Parameters for the Two Material Zones

Zone	D	Σ_a	$\Sigma_S = \Sigma_T - \Sigma_a$
Z_1	0.33333	0.1	0.9
Z_2	0.37037	0.2	0.7

We ran the SND code on a spatial grid consisting of one node per layer and the results for the scalar flux profile as generated with the present spatial reconstruction are presented in Fig. 3, where we used a step of 0.01cm to build the graph.

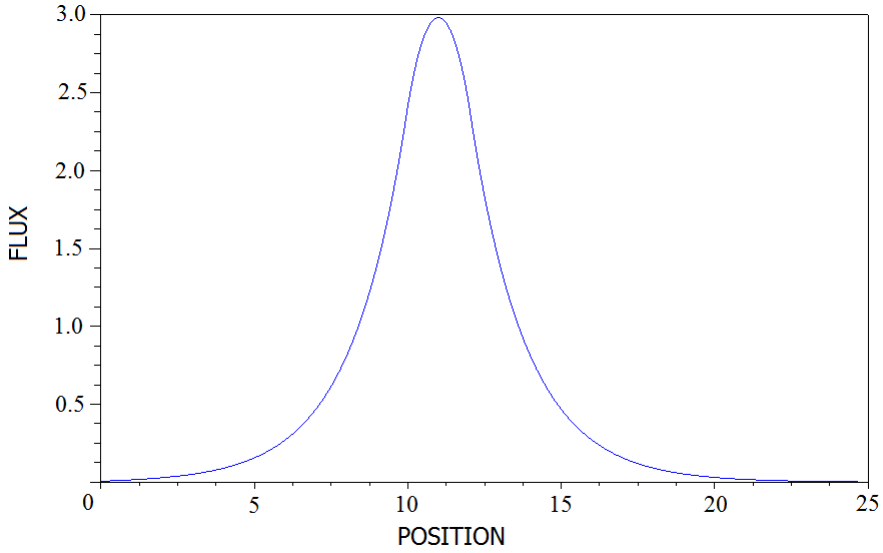

Figure 3. Spatial reconstruction for the scalar flux profile.

The numerical results generated by the angular synthetic reconstruction are listed in Table 3. In the first column of the table, we present various positions of the domain where the angular flux were calculated in several directions, positive and negative, of the conventional Gauss-Legendre S_{16} angular quadrature [2], that are listed in the second column of Table 3.

Table 3. Numerical results generated by the synthetic angular reconstruction

Position x (cm)	Direction (S_{16})	Reconstructed Angular Flux	DD-S_{16} [a]	Relative Deviation (%)
5	-0.8656312	0.1317675	0.1259	4.66
7	-0.7554044	0.3525338	0.3304	6.70
8	0.4580168	0.2903192	0.2697	7.65
11	0.8656312	1.3343402	1.3536	1.42
13	0.7554044	0.9911340	0.9648	2.73
15	0.9894009	0.4157411	0.3931	5.76
20	0.0950125	0.0143002	0.0149	4.03
Execution Time:		0.165 seconds	106.5 seconds	

a. Diamond Difference – Gauss-Legendre S_{16} [4].

The third column of Table 3 lists the numerical values for the angular flux generated by the offered synthetic diffusion angular reconstruction method and the fourth column we have the

numerical values generated by the *Diamond Difference* (DD) method using the Gauss-Legendre S_{16} angular quadrature [2]. As we see in the fifth column, the percentage relative deviations were generally very small, and the maximum value of 7.65% occurred at position 8cm and in the direction $\mu = 0.4580168$.

4. DISCUSSION

The SND method generates numerical solution with no spatial truncation errors for one-speed slab-geometry diffusion problems, regardless of the spatial grid set up on the domain, but apart from computational finite arithmetic considerations. Therefore, one may be able to solve slab-geometry one-speed diffusion problems with many fewer spatial cells than standard numerical methods, e.g., the finite-difference method. On the other hand, as a drawback of coarse-mesh numerical methods, we note that they do not generate localized quantities that frequently are needed, as the grid points may be considerably away from each other. Therefore, we have described in this paper two numerical algorithms to reconstruct the coarse-mesh solution within each discretization spatial node, i.e., the spatial reconstruction scheme and the synthetic angular reconstruction scheme. According to the numerical results generated for the model problem considered in the previous section by the present reconstruction schemes, we conclude that they are reasonably accurate with respect to the direct calculations. In addition, as we see in the last row of Table 3, the offered synthetic angular reconstruction scheme generates accurate results in much less computational running time than the DD-S_{16} method. However, we remark that for highly absorbing multilayer slabs, the present synthetic angular reconstruction scheme may not generate accurate results since diffusion theory is not a good model for such problems.

As future work we suggest to implement this concept to energy-dependent problems. We plan to report on the multigroup reconstruction schemes after they have been implemented and fully tested.

ACKNOWLEDGMENTS

This work was supported by Conselho Nacional de Desenvolvimento Científico e Tecnológico (CNPq – Brazil) and Fundação Carlos Chagas Filho de Amparo à Pesquisa do Estado do Rio de Janeiro (FAPERJ – Brazil). The authors thank Emilio Jorge Lydia for running his code DD-S_{16}.

REFERENCES

1. J.J. Duderstadt and L.J. Hamilton, *Nuclear Reactor Analysis*, John Wiley & Sons, New York (1976).
2. E.E Lewis and W.F. Miller Jr., *Computational Methods of Neutron Transport*, American Nuclear Society, IL (1993).
3. R.L. Burden and J. D. Faires, *Numerical Analysis*, Prindle, Weber & Schmidt (1985).
4. E. J. Lydia, private communication.
5. SCILAB homepage: www.scilab.org.